GEODYNAMICS & TECTONOPHYSICS
Published by the Institute of the Earth's Crust, Siberian Branch, Russian Academy of Sciences

TECTONOPHYSICS

2023 VOLUME 14 ISSUE 6 ARTICLE 0725

ISSN 2078-502X

DOI: 10.5800/GT-2023-14-6-0725

MODELS FOR THE FORMATION OF POLYPHASE GABBRO-MONZODIORITE MASSIFS OF THE WESTERN SANGILEN IN THE COLLISIONAL AND TRANSTENSIONAL-SHEAR SETTINGS

A.N. Semenov ✉, **O.P. Polyansky**

Sobolev Institute of Geology and Mineralogy, Siberian Branch of the Russian Academy of Sciences, 3 Academician Koptyug Ave, Novosibirsk 630090, Russia

ABSTRACT. A model for the formation of intrusions of the collision stage of 525–490 Ma and a model of magmatism of the transtensional shear stage of 465–440 Ma within the Mugur-Chinchilig and Erzin-Naryn blocks of Western Sangilen (Tuva) have been developed to describe the process of crust-mantle interaction. Model experiments confirm petrological data on the presence of multi-level chambers during the formation of the Pravotarlashkinsky and Bashkymugur massifs. The proposed model describes the migration of mantle magmas above the head of the mantle plume at the collision stage and assumes the rise of magmas along a permeable tectonic zone in the mantle lithosphere and crust at the transtensional-shear stage. The modeling results allow us to establish that material from the magma chamber can reach depths of the upper crust in the volume ratio of gabbroids to diorites from 1 : 2 to 3 : 4 and additionally introduce about 5 % of the volume fraction of lower crustal material.

The physical parameters of the primary magmas (viscosity, solidus and liquidus temperatures, degree of melting depending on temperature and composition, change in density) were calculated taking into account the real geochemical characteristics of igneous rocks from the polyphase massifs of Western Sangilen.

KEYWORDS: thermomechanical model; melting; magma chamber; numerical modeling; Sangilen; gabbro-diorite intrusion; thermal aureole

FUNDING: The study was funded by the grant of the Russian Science Foundation (project 22-77-00068).

RESEARCH ARTICLE

Correspondence: Alexander N. Semenov, semenov@igm.nsc.ru

Received: Aril 6, 2023
Revised: May 10, 2023
Accepted: May 12, 2023

FOR CITATION: Semenov A.N., Polyansky O.P., 2023. Models for the Formation of Polyphase Gabbro-Monzodiorite Massifs of the Western Sangilen in the Collisional and Transtensional-Shear Settings. Geodynamics & Tectonophysics 14 (6), 0725. doi:10.5800/GT-2023-14-6-0725

1. INTRODUCTION

The processes of interaction between mantle and crustal magmas are actively discussed in petrological and geochronological aspects. At the same time, the thermo-mechanical and rheological aspects of the processes of segregation and extraction of melts, as well as the mechanisms of magma transport to the middle and upper crustal levels remain controversial. Different mechanisms of functioning of magma-plumbing systems are considered: a) migration of melts along tectonically weakened, permeable, fractured channels [Keller et al., 2013], b) crustal or mantle magmatic diapirism and advection [Schmeling et al., 2019], c) thermo-mechanical erosion of the roof of the magma chamber and capture of surrounding material by magma [Marsh, 1982]. In the listed mechanisms, the "space problem" is solved in different ways. In fracture intrusions, migration channels appear before magma enters there, or the melt itself, due to the compressibility of the host medium, creates a permeable channel [Babichev et al., 2014]. During diapirism, it is believed that a less dense magmatic core rises through a plastic heated mass of host rocks [Cruden, Weinberg, 2018]. In the third case, it is assumed that the penetration of magma occurs under conditions of a balance between the volume of eroded and contaminated matter.

One of the well-studied objects of interaction between mantle magma and crustal wall rocks are the ultramafic-mafic massifs of the West Sangilen block (Tuva), synchronous with contact and regional plutonometamorphic complexes (Fig. 1).

The purpose of this work: on the example of intrusive and metamorphic complexes of Western Sangilen, using the numerical modeling method, to propose realistic mechanisms for the formation of a system of multi-level chambers and the formation of polyphase massifs that arose in different geotectonic settings.

2. GEOLOGICAL SETTING AND EMPLACEMENT STAGES

Petrological and geochronological data on metamorphic and igneous associations of the Sangilen block, which is part of the structure of the Tuva-Mongolian continent (TMC), point to an independent Cambrian-Ordovician accretion-collision stage (510–440 Ma) [Gibscher et al., 2017]. Reconstruction of tectonic history was carried out using tectonic and geochronological data [Vladimirov et al., 2005, Gibscher et al., 2017]; geological and petrological data on magmatism and metamorphism of the region [Gibsher et al., 2012; Izokh et al., 2001; Kargopolov, 1997; Karmysheva et al., 2019; Shelepaev et al., 2018], as well as the results of numerical modeling [Polyansky et al., 2019, 2021b].

The tectono-metamorphic and geodynamic evolution of the Sangilen block represents a change in tectonic regimes, marked by thermal events and manifestations of different ages and different types of ultramafic-mafic and granitoid associations [Vladimirov et al., 2005; Kozakov, Azimov, 2017; Shelepaev et al., 2018] (Fig. 2). Within the Western Sangilen block, several stages of formation of gabbro-monzodiorite massifs that arose in different geodynamic settings are recorded. In recent years, a large number of ages of intrusion emplacement between from 570 to 440 Ma related to the Cambro-Ordovician accretion-collision stage have been carried out [Petrova, Kostitsyn, 1997; Kozakov et al., 1999, 2001; Izokh et al., 2001; Vladimirov et al., 2005; Kuznetsova et al., 2021]: 570–535 Ma corresponds to the accretion-island arc regime; 535–495 Ma corresponds to the formation of the Sangilen collision system as a result of the convergence of the margin of the TMC and the Tannuol island arc, the introduction of syncollisional mafic melts with accompanying high-gradient granulite metamorphism; The post-collisional transtensional shear regime lasted in the range of 495–430 Ma [Vladimirov et al., 2005]. At the final strike-slip stage of the collision, the gabbro-monzodiorite Bayankol (496±3 Ma [Izokh et al., 2001]) and Erzinsky (490±10 Ma [Kozakov et al., 1999]) intrusions were formed. The intrusion and formation of the Bashkymugur websterite-gabbro-monzodiorite complex (465±1.2 Ma [Izokh et al., 2001]) occurred against the background of late collisional extension and collapse of the orogen. A feature of this stage is the manifestation of high-temperature zoned metamorphic complexes, including shallow granulites [Kargopolov, 1997; Fedorovsky et al., 1995]. At the same time, various ultrabmafic-mafic associations appeared in Western Sangilen, synchronous with metamorphic formations of the HT/LP type (high temperatures/low pressures) with a wide contact-metamorphic zoning [Izokh et al., 2001].

The composition and sequence of magmatism pulses in the history of the formation of specific complexes have been characterized in detail [Gibsher et al., 2012; Shelepaev et al., 2018]. As a rule, the massifs have a two-phase structure with the first gabbroic phase and the second monzodiorite phase (Bayankol, Bashkymugur, Erzin massifs). The area of monzodiorite outcrops exceeds the area of distribution of gabbroids in the indicated massifs. The model objects of this study are the Bashkymugur websterite-gabbro-monzodiorite massif with the surrounding Mugur zonal metamorphic complex and the Bayankol gabbro-monzodiorite massif.

The Bayankol gabbro-monzodiorite massif consists of several separate sheet-like undifferentiated gabbro bodies that differ in melanocratic content. The massif has a two-phase structure: the first phase is gabbroids, the second is monzodiorites. Near-contact partial melting is characteristic of intrusive contacts of monzodiorites and olivine gabbronorites in the sags of the roof of the Bayankol massif. In direct contact, the phenomena of mixing (mingling) of felsic and mafic melts with the formation of hybrid rocks are observed. The age of the massif is 496.5±3.6 Ma according to the U-Pb method [Kozakov et al., 1999] and 489 ±3 Ma according to the Ar-Ar method [Shelepaev et al., 2018]. Gabbroids and monzodiorites are intruded by granodiorites with an age of 487±2 – 488±3 Ma [Smolyakova et al., 2021].

Previous studies have shown that the area of Western Sangilen shows signs of several metamorphic events: M1

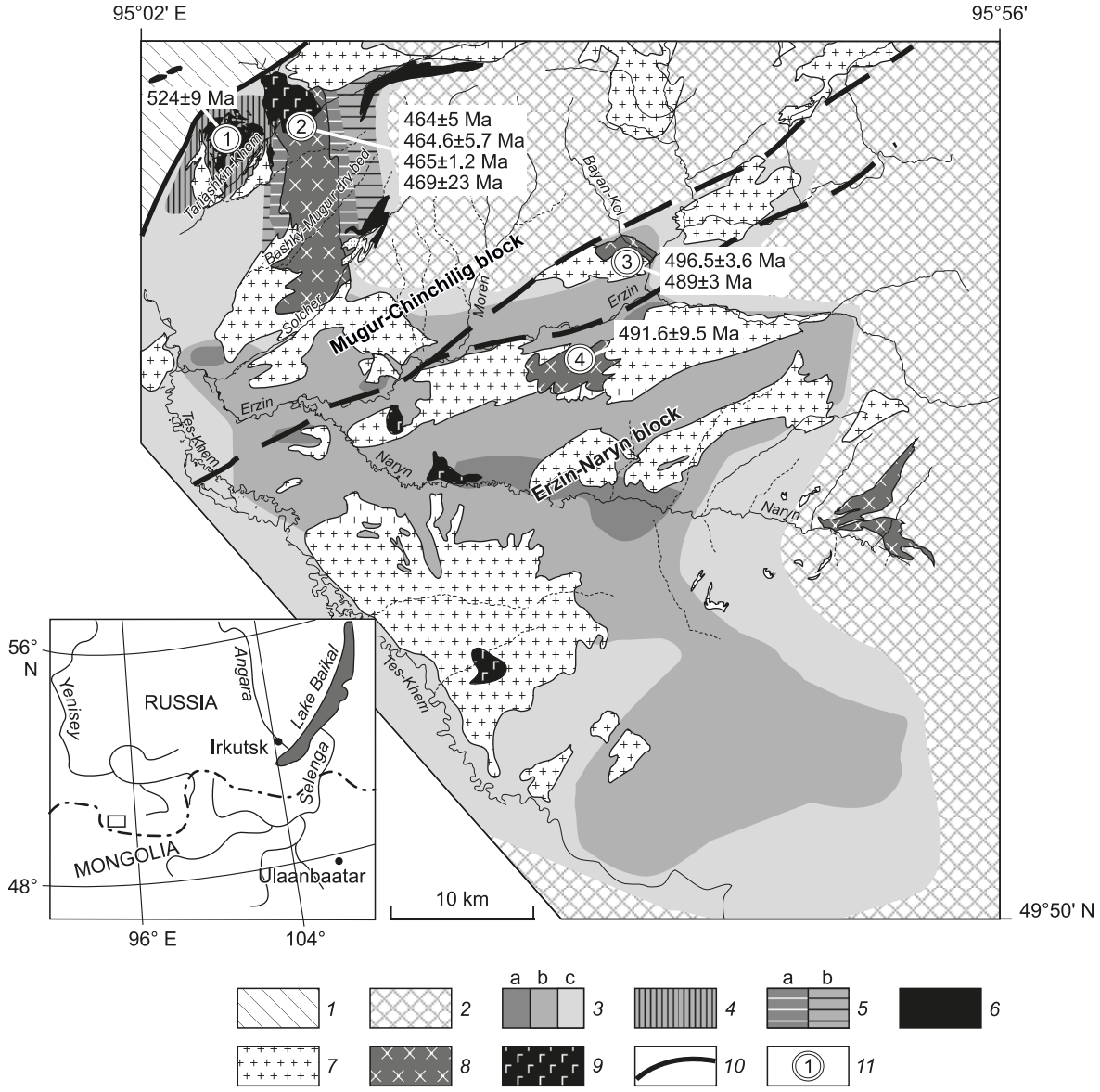

Fig. 1. Scheme of the structure of the Western Sangilen (Southeastern Tuva) after [Vladimirov et al., 2005; Izokh et al., 2001; Kargopolov, 1997].

1 – Vendian – Early Cambrian metavolcanics of the Agar-Dag suture zone; *2* – aureole of Barrovian (Ky-schist) metamorphism M1; *3* – regional metamorphic formations with an age of 490 Ma: a – Hyp-, b – Sil-, c – And-zones; *4* – two-Px and Sil-Kfs hornfelses of the contact aureole of the Pravotarlashka massif; *5* – metamorphic formations from the contact aureole of the Bashky-Mugur massif: a – Hyp-, b – Sil-zones; *6* – ultrabasites; *7* – granites; *8* – diorites and monzodiorites; *9* – differentiated gabbroids; *10* – Agar-Dag fault; *11* – gabbroid intrusives (circled numbers): 1 – Pravotarlashka troctolite-anorthosite-gabbro, 2 – Bashky-Mugur websterite-gabbronorite-monzodiorite, 3 – Bayan-Kol gabbro-monzodiorite, 4 – Erzin gabbro-monzodiorite. The bold dotted line is the Erzin strike-slip zone separating the Mugur-Chinchilig and Erzin-Naryn blocks.

metamorphism of the Barrow type with an age of 515 Ma [Gibscher et al., 2017], and two stages of high-gradient metamorphism M2 associated with the intrusion of gabbro-monzodiorite intrusions (approx. 490 and 465 Ma), the differentiation of which took place in intermediate chambers at different depths. Geothermobarometry data on metamorphic rocks of contact aureoles, as well as mineral parageneses and compositions of minerals of igneous complexes indicate that the formation of gabbro-monzodiorite massifs of Western Sangilen occurred at different depths [Kargopolov, 1997; Egorova et al., 2006]. The crystallization parameters of ultramafic-mafic intrusions and the conditions of metamorphism for the Cambro-Ordovician collision orogen, according to the authors, allow us to speak about three levels of emplacement.

According to the study of gabbroic xenoliths, including garnet-bearing ones, from alkali-basaltic dikes of the Agardag complex, cutting through the rocks of the Bashky-mugur and Pravotarlashkinsky massifs, a system of multi-depth intrusive chambers is established [Egorova et al., 2006] (Fig. 3). Data from thermobarometric estimations carried out on the compositions of gabbroic xenoliths indicate

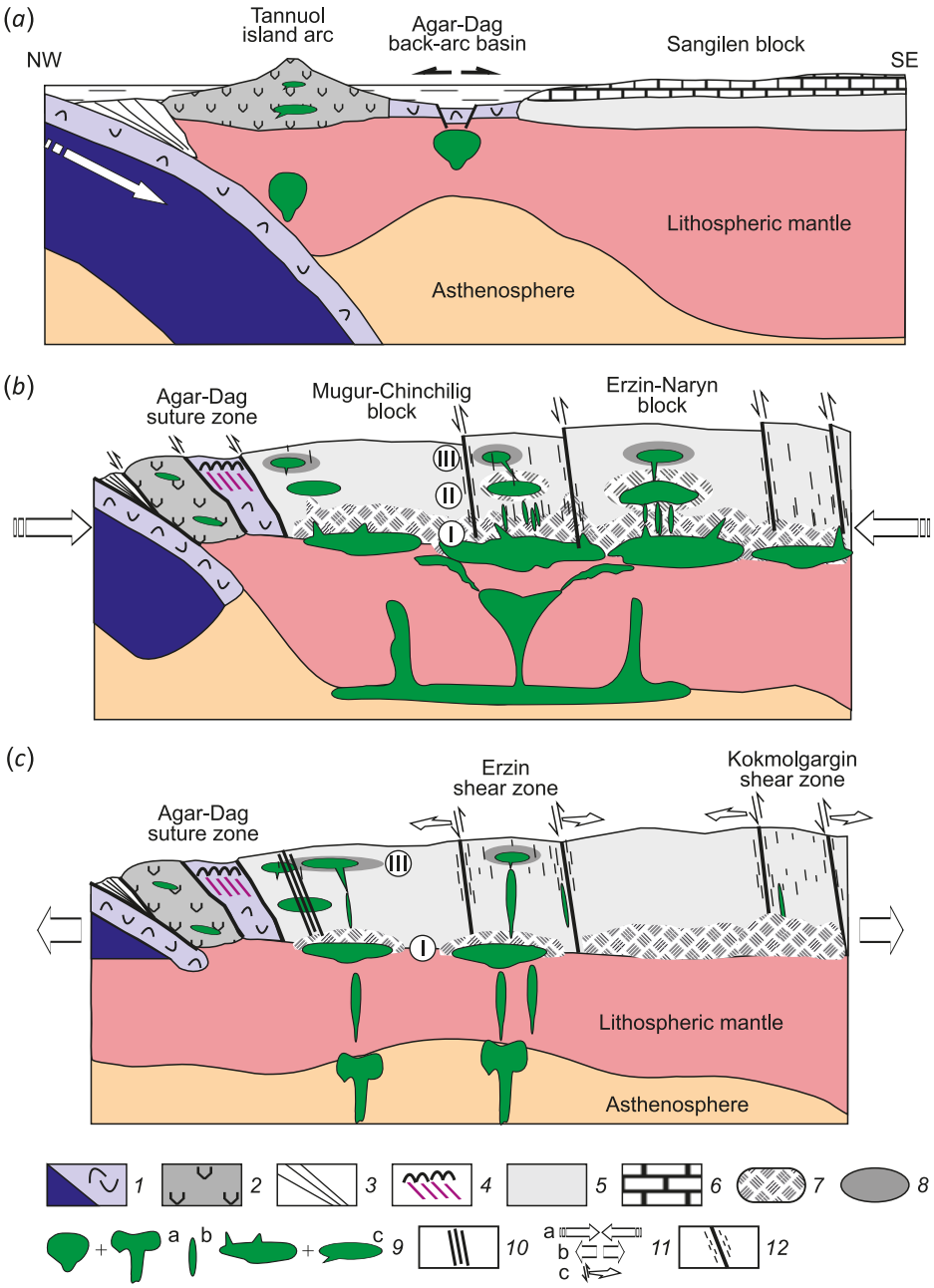

Fig. 2. The tectonic history reconstruction reflecting the processes of basite magmatism and associated metamorphism of the early Caledonides of the Sangilen block on the western margin of the Tuva-Mongolian continent over three age intervals.
Performed using the tectonic and geochronological data [Vladimirov et al., 2005, 2017; Gibsher et al., 2017], geological and petrological data on regional magmatism and metamorphism [Gibsher et al., 2012; Izokh et al., 2001; Kargapolov, 1997; Karmysheva et al., 2019; Shelepaev et al., 2018], and numerical modeling results [Polyansky et al., 2021b]: (*a*) – 570–520 Ma – accretionary-subduction regime; (*b*) – 535–495 Ma – the formation of the Sangilen collisional system as a result of the convergence of the TMK margin with the Tannuol island arc, the intrusion of syn-collisional mafic melts with concomitant high-gradient granulite metamorphism; (*c*) – 495–430 Ma – transtensional regime, formation of shallow intrusions, granulite metamorphism of the HT/LP type.
1 – oceanic crust and lithospheric mantle; *2* – Tannuol island arc; *3* – accretionary prism; *4* – ophiolites of the Agar-Dag zone; *5* – metamorphic complexes of the Sangilen block crust – Grt-St-Ky schists of M1 stage, Ky-Sil type; *6* – carbonates of the Sangilen block cover; *7–8* – areas of high-gradient metamorphism (M2): *7* – UHT granulite metamorphism (M2) in the lower/middle crust, *8* – granulite zone of HT/LP metamorphism (M2) in the upper crust (And-Sil type); *9* – mantle mafic melts: a – magma generation areas, b – magma conduits, c – intrusive chambers; *10* – dikes of the Agar-Dag alkaline-basaltoid complex; *11* – geodynamic regimes: a – collisions, b – extensions, c – extensions with shear; *12* – faults and mingling dikes. I–III – lower-, middle-, and upper-crustal levels of intermediate mafic chambers.

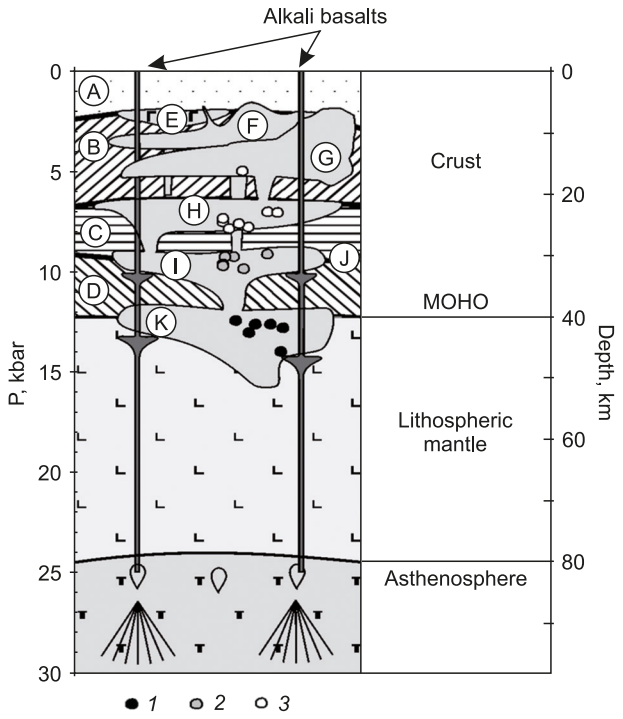

Fig. 3. Schematic section of the lithosphere of the western part of the Sangilen Plateau in the Late Ordovician after [Egorova et al., 2006].
A – Cambrian volcanic-sedimentary complex; B – Morena metamorphic complex; C, D – lower crustal areas; E – position of the Pravotarlashka intrusion; F – gabbroids of the Bashky-Mugur massif; G – monzodiorites of the Bashky-Mugur massif; H, I, J – inferred intermediate magma chambers according to the thermobarometric data; K – boundaries of the crustal layers. *1–3* – pressures for gabbroid massifs estimated from variously composed xenoliths of the Agardag dike complex.

the presence of intermediate mafic chambers at different depths. Pressures determined for garnet gabbros are 10–12 kbar (37–44 km). Garnet-free gabbroids (group 2) were formed at lower pressures (8–10 kbar), corresponding to depths of 30–33 km. The formation of gabbroids with low alumina content in pyroxenes (group 3) occurred at shallow depths of 10–20 km (3–6 kbar), close to the level of formation of the Bashkymugur and Pravotarlashkinsky massifs, for which the pressure is estimated at 2–3 kbar based on the host hornfels [Kargopolov, 1991] and 2–5 kbar according to the Cpx barometer [Nimis, 2002]. The calculated equilibrium temperatures of mineral associations of gabbroids of all groups range from 950 to 1100 °C. Mid-crustal intrusions, as a rule, are undifferentiated (Erzinsky and Bayankol massifs at the stage of 490 Ma) at a level of P=4–5 kbar [Karmysheva et al., 2019] or P=7–8 kbar (26–30 km) [Selyatitskii et al., 2021]. Shallow intrusions (P=2–4 kbar, 7–14 km) are represented by the Pravotarlashkinsky massif at the stage of 524±9 million years [Shelepaev et al., 2018] and Bashkymugur at the stage of 465 Ma [Izokh et al., 2001; Kargopolov, 1991].

The Bashkymugur websterite-gabbro-monzodiorite massif is a large multiphase body elongated in the meridional direction (5×17 km) (Fig. 4). The first phase is represented by gabbroids, which form a body (3×4 km) in the northern part of the Bashkymugur massif. It shows layering and differentiation, which is expressed in the appearance of horizons and individual layers composed of pyroxenites and melanocratic gabbronorites in the lower parts of the massif, and leucocratic gabbro and anorthosites predominate in the upper part of the intrusion. The second phase – the main part of the rocks of the Bashkymugur massif – is represented by uniformly grained biotite-amphibole quartz monzodiorites. The age of the massif is 464±5.7 million years according to the U-Pb method [Kozakov et al., 1999] and 465±1.2 million years according to the Ar-Ar method [Shelepaev et al., 2018], the age of introduction of individual phases is indistinguishable by geochronological dating.

3. PHYSICAL PROPERTIES OF MAGMAS

To correctly formulate a mathematical model, a quantitative description of all physical properties of materials in the range of possible temperatures in both the solid and partially molten states is required. Density, degree of crystallinity, as well as solidus and liquidus temperatures were calculated using the MELTS program [Gualda et al., 2012; Ghiorso, Gualda, 2015] taking into account the actual compositions of igneous rocks. The compositions of igneous rocks of ultramafic-mafic massifs used in the calculations are presented in Table 1 [Shelepaev et al., 2018].

The viscosity of the melts was calculated from experimental dependences, taking into account the bulk chemical composition of the rocks, temperature and degree of crystallization, according to the dependence obtained in [Persikov, Bukhtiyarov, 2009].

$$\mu_T^P = \mu_0 \exp\left(\frac{E_x^P}{RT}\right),$$

$$\mu_{ef} = \mu_T^P \left(1 - V_{cr}\right)^{-3.35} \left(1 - 1.5V_{liq}\right)^{-0.55},$$

where μ_T^P – melt viscosity at given temperature and pressure; μ_0 – constant characterizing melt viscosity at $T \to \infty$, $\mu_0 = 10^{-3.5} \pm 10^{0.1}$ (0.1 Pa·s); T – absolute temperature (K); E_x^P – activation energy of viscous flow which is a function of pressure and composition of melts including volatiles; R – universal gas constant; $0 \le V_{cr} \le 0.45$, $0 \le V_{liq} \le 0.45$ – volume fraction of crystals and gaseous phase, respectively.

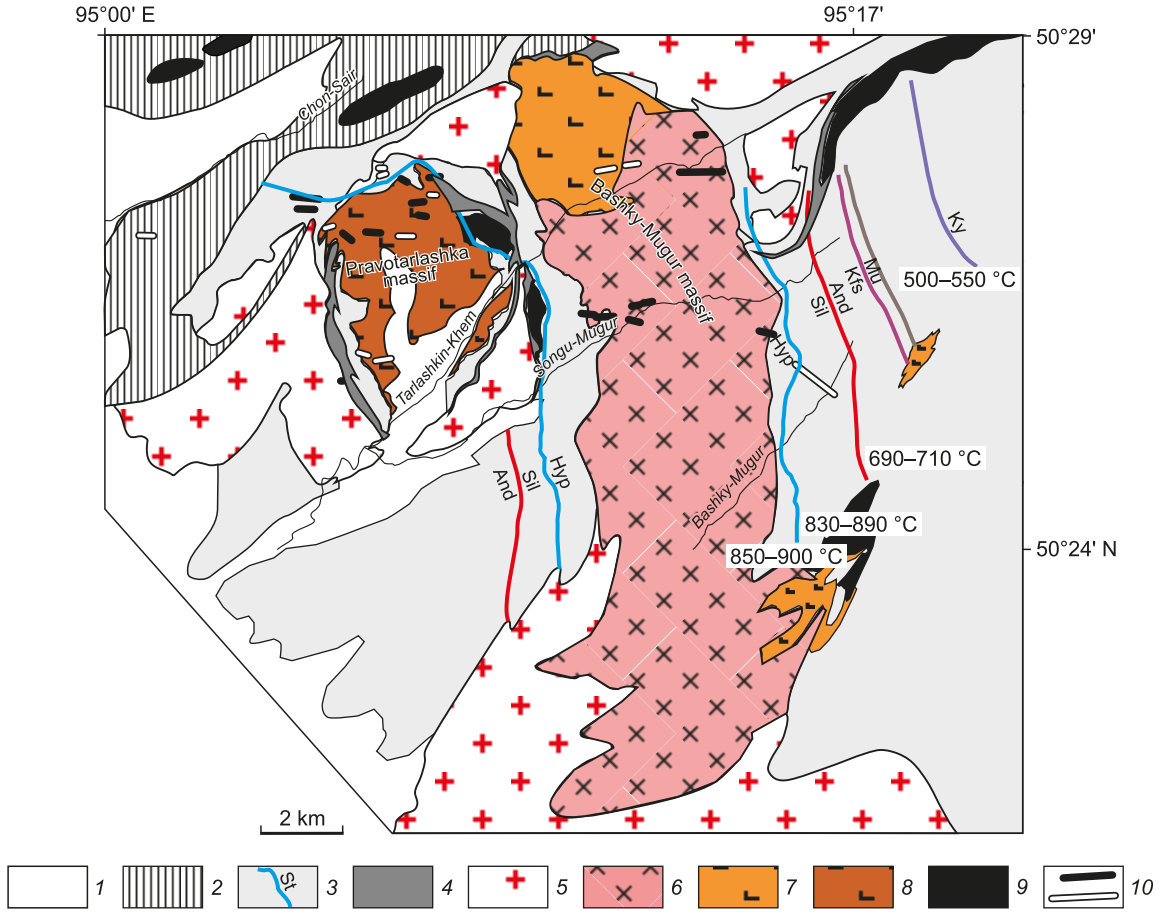

Fig. 4. Geological structure and contact-metamorphic zonality of the Bashky-Mugur and Pravotarlashka massifs after [Kargopolov, 1997] and [Gibsher et al., 2012], with changes.
1 – Quaternary and Neogene deposits; *2* – metabasites and volcanic-sedimentary rocks of the Agardag complex; *3* – shales and gneisses of the Mugur-Teshem complex with metamorphism isograds, mineral symbols are displayed in places of mineral occurrences; *4* – amphibolite and metavolcanic horizons of the Mugur-Teshem complex; *5* – granites; *6–7* – monzodiorites of the second phase (*6*) and gabbroids of the first phase (*7*) of the intrusion of the Bashky-Mugur massif; *8* – gabbroids of the Pravotarlashka massif; *9* – ultrabasic rocks of the Agardag ophiolite complex; *10* – two types of camptonite dikes of the Agardag complex.

Table 1. Chemical composition (wt. %) of basite massifs of the Western Sangilen

Massif	Bayan-Kol					Erzin			Bashky-Mugur			
Sample	Ш3	Ш25	И17	СН40	СН75	Ш28	Т166	Ш26	И71	Ш7/1	И64/1	Ш16
SiO_2	45.52	46.84	49.78	57.89	49.07	46.22	48.81	52.49	45.93	49.31	49.83	59.77
TiO_2	0.56	1.8	2.02	0.71	2.44	0.49	2.31	1.32	0.37	0.35	1.31	0.88
Al_2O_3	6.51	15.46	18.77	17.02	16.63	13.03	14.51	15.15	15.79	18.7	17.8	16.1
Fe_2O_3	10.46	9.55	10.72	6.24	12.07	13.34	13.01	10.43	13.04	5.33	11.39	6.81
MnO	0.17	0.15	0.18	0.12	0.21	0.21	0.201	0.22	0.23	0.11	0.19	0.14
MgO	24.74	12.14	3.96	4.31	4.46	14.01	6.08	4.8	12.84	12.18	7.25	2.58
CaO	8.64	9.69	8.39	7.72	6.75	9.42	8.18	8.21	9.02	16.83	8.46	5.3
Na_2O	1.29	1.96	3.72	2.75	4.27	1.51	3.2	4.48	1.63	2.31	2.37	4.61
K_2O	0.51	0.4	0.28	1.55	2.39	0.23	0.8	1.61	0.2	0.22	1.17	2.55
П.п.п	1.06	2.48	1.5	0.58	0.93	0.28	1.26	0.54	0.2	0.71	0.12	0.38
Сумма	99.4	99.4	99.8	99.04	100.26	98.8	98.3	99.5	99.3	100	100.1	99.4

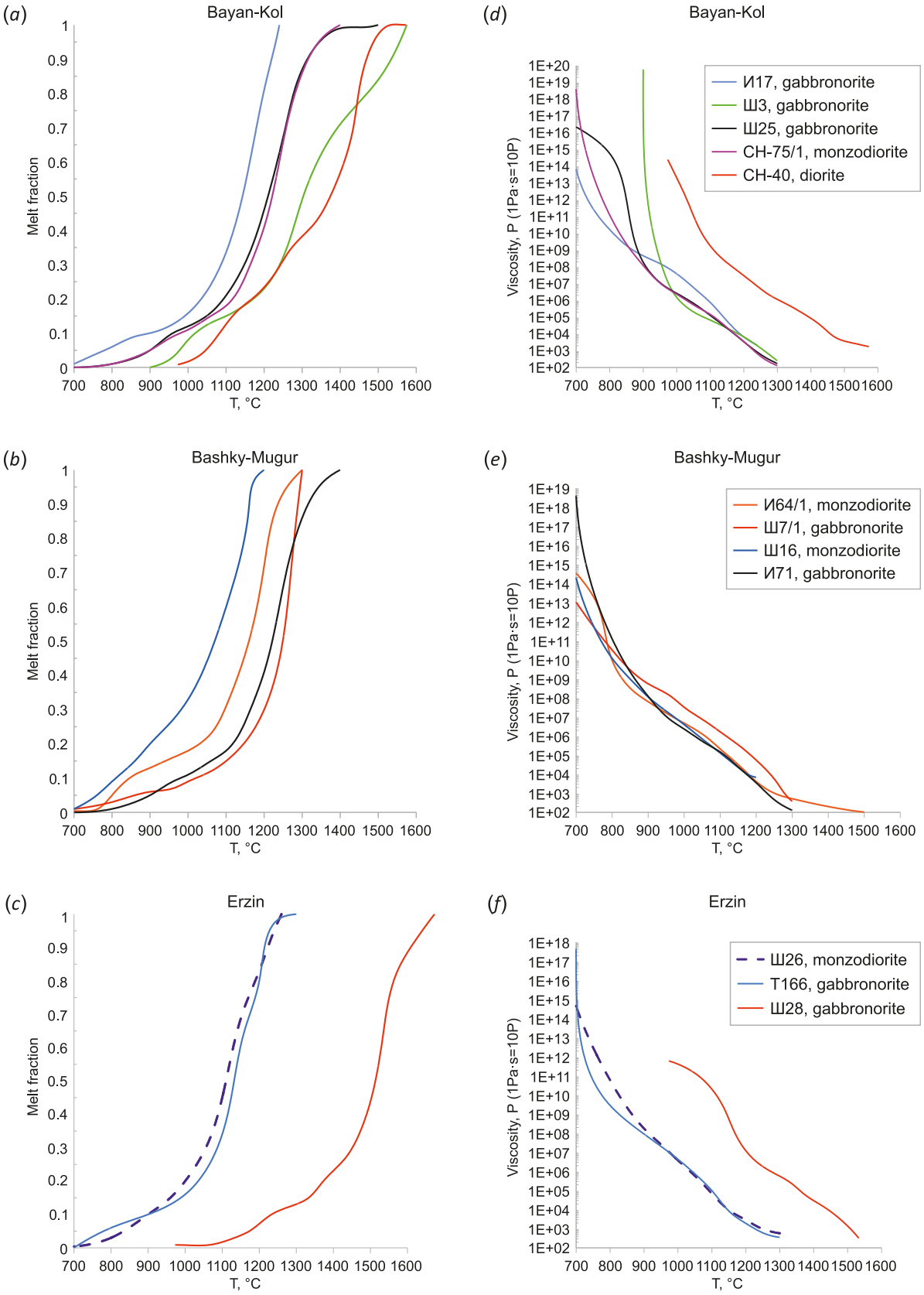

Fig. 5. Melt fraction (*a, b, c*) in the solidus-liquidus temperature range, calculated using the MELTS software package [Ghiorso, Gualda 2015], and viscosity of magmas (*d, e, f*), calculated from experimental dependences [Persikov, Bukhtiyarov, 2009] taking into account bulk chemical composition, temperature and fraction of crystalline matter at pressure *P=7* kbar and identical content of H_2O=2 wt. %, for representative rocks of the Bayan-Kol, Bashky-Mugur and Erzin massifs (*b*).

The temperature dependences of the melt fraction (Fig. 5, a, b, c) and viscosity (Fig. 5, d, e, f) were obtained at a pressure P=7 Kbar and a water content of 2 wt. %. The dependence of these parameters on the differences in the compositions of monzodiorites and gabbronorites for all massifs can be traced. In addition, for example, the gabbronorites of the Bayankol massif (samples И17, Ш3 and Ш25), with approximately the same SiO_2 content, differ in the degree of melting (melt fraction) by up to 40 % at the same temperature. Apparently, the reason for this is strong variations in magnesium content: in some rocks the MgO content reaches 24–25 %, which characterizes them as picrites (Fig. 5, a). The greatest difference in melting temperatures is achieved in rocks of different phases of intrusion of the Erzin massif, a moderate scatter is recorded for the Bayankol massif, and the smallest for the Bashkymugur massif. Melt fraction curves are non-monotonic, which is determined by the sequential crystallization of minerals. According to the melting diagrams of diorites and gabbroids of igneous complexes (Fig. 5), which differ in silica content and magnesium content, it is clear that the same degree of melting is achieved at an elevated temperature of 200–400 °C.

A similar scatter of magma viscosity values, from maximum to minimum, is observed in the series of the Erzin – Bayankol – Bashkymugur igneous massifs (Fig. 5, d, e, f). By jointly analyzing the curves of the degree of melting and magma viscosity depending on temperature, we can conclude that viscosity is affected by both the composition of magmas (primarily the silica content) and the melting temperature. The dependence of the decrease in the viscosity of melts in the series from acidic to ultrabasic [Persikov, 1984] becomes opposite in the same series when taking into account the degree of crystallinity upon cooling in the same temperature range. Thus, high-magnesium gabbronorites of the Erzin massif (sample Ш28, Fig. 5, c) turn out to be more viscous than monzodiorites (sample Ш26) at the same temperature due to a higher degree of crystallization (Fig. 5, f).

It should be noted that the viscosity dependence according to [Persikov, Bukhtiyarov, 2009] was developed for subliquidus magmatic melts and is less suitable for near-solidus magmas. The rheology of crust and mantle matter in a subsolidus or partially molten state is characterized by the creeping flow equation. In thermomechanical modeling, the flow law was used according to the experimental dependence [Mei et al., 2002], which describes the non-Newtonian, temperature-dependent "effective" viscosity:

$$\eta = \exp\left(\frac{-c\phi}{n}\right) A^{\frac{-1}{n}} \left[\dot{\varepsilon}_{II}\right]^{\frac{1-n}{n}} \exp\left(\frac{H}{nRT}\right),$$

where T – temperature; $\dot{\varepsilon}_{II}$ – strain rate; ϕ – melt fraction during melting, n; A, H – rheological parameters of the material of the crust, mantle and magma (Table 2).

4. MODEL DESCRIPTION AND THERMOPHYSICAL PARAMETERS

Two models for the formation of massifs of the Western Sangilen block have been developed, characterizing the magmatism of the accretion-collision and transtensional stages, shown in Fig. 3, b and 3, c, respectively. The magmatic process is described within the framework of a numerical thermomechanical model of the system "magma chamber – magma transport – formation of intermediate chambers – pluton emplacement". The occurrence of a deep magma chamber in the models is assumed to be "instantaneous", which is a slight simplification of the description of the real process, but does not have a significant impact on the subsequent evolution of the magmatic system.

In the model of magmatism of the accretion-collision stage, it is assumed that the magma chamber arose in the upper mantle under a collisional orogen [Shelepaev et al., 2018] (see Fig. 2, a, stage 570–520 Ma,). The magma chamber is assumed to be in the form of a layer 10 km thick and 45 km long and located in the upper mantle at a depth of 80 km, in the transition region of spinel/garnet peridotite stability (Fig. 6, a) (see Chapter 7). It is assumed that the volume of the magma chamber is reduced during the process of melt extraction. The boundary conditions at the boundaries of the magma reservoir are as follows: the condition of an impenetrable adiabatic wall is set on the side boundaries, and the condition of an impenetrable boundary with a fixed temperature is set on the lower boundary. The magma chamber is filled with mafic melt with a density of 2700–2800 at an initial temperature T_0= =1200 °C.

The model of the transtensional stage assumes the presence of a suture between tectonic blocks, which is a permeable feeder channel from the deep magma chamber to the base of the crust (Fig. 6, b). It is allowed to replenish the magma chamber with a melt at a constant temperature, maintaining excess pressure in the chamber. The roof and

Table 2. Physical properties of substances and creep flow law parameters

Parameters	C_P, J/(kg-K)	K, W/(m–K)	n	A, Pa^{-n}/s	H, kJ/mol
Crust*	1250	2.5	2.6	4E-21	134000
Mantle**	1250	3.5	3.35	1E-16	540000
Basites, monzodiorites***	1250	2.5	3.05	6.3E-20	276000

Note. * – [Kronenberg, Tullis, 1984], ** – [Chopra, Patterson, 1984], *** – [Carter, Tsenn, 1987].

bottom of the chamber are permeable for the transport of melts; the condition of a rigid wall is met at the lateral boundaries of the chamber. In areas of the base outside the chamber, conditions of an impenetrable fixed boundary and a constant temperature of 600 °C are imposed. The temperature in the crust at the initial moment of time is set linearly from 0 to 600 °C. This model assumes the presence of magma differentiated in composition, consisting of monzodiorite (more fusible) and mafic components. The process of magma differentiation in the chamber itself is not considered in the model. A linear increase in density is accepted from 2520 to 2680 kg/m^3 in the liquidus-solidus temperature range of 1200–900 °C for monzodiorite and from 2700 to 2800 kg/m^3 at T=1200–1000 °C for basaltic magma.

The petrological model of the crust composition is considered in a simplified form. The model crust is divided into lower (granulite), middle (granodiorite) and upper (metapelitic) layers. The three-layer structure of the crust of the Sangilen terrane is accepted according to the density model of the eastern part of the Altai-Sayan region, built on the basis of seismological and gravitational data [Vasilevsky et al., 1985]. Following [Bea, 2012], the degree of "fertility" of the crust (in terms of the content of fusible

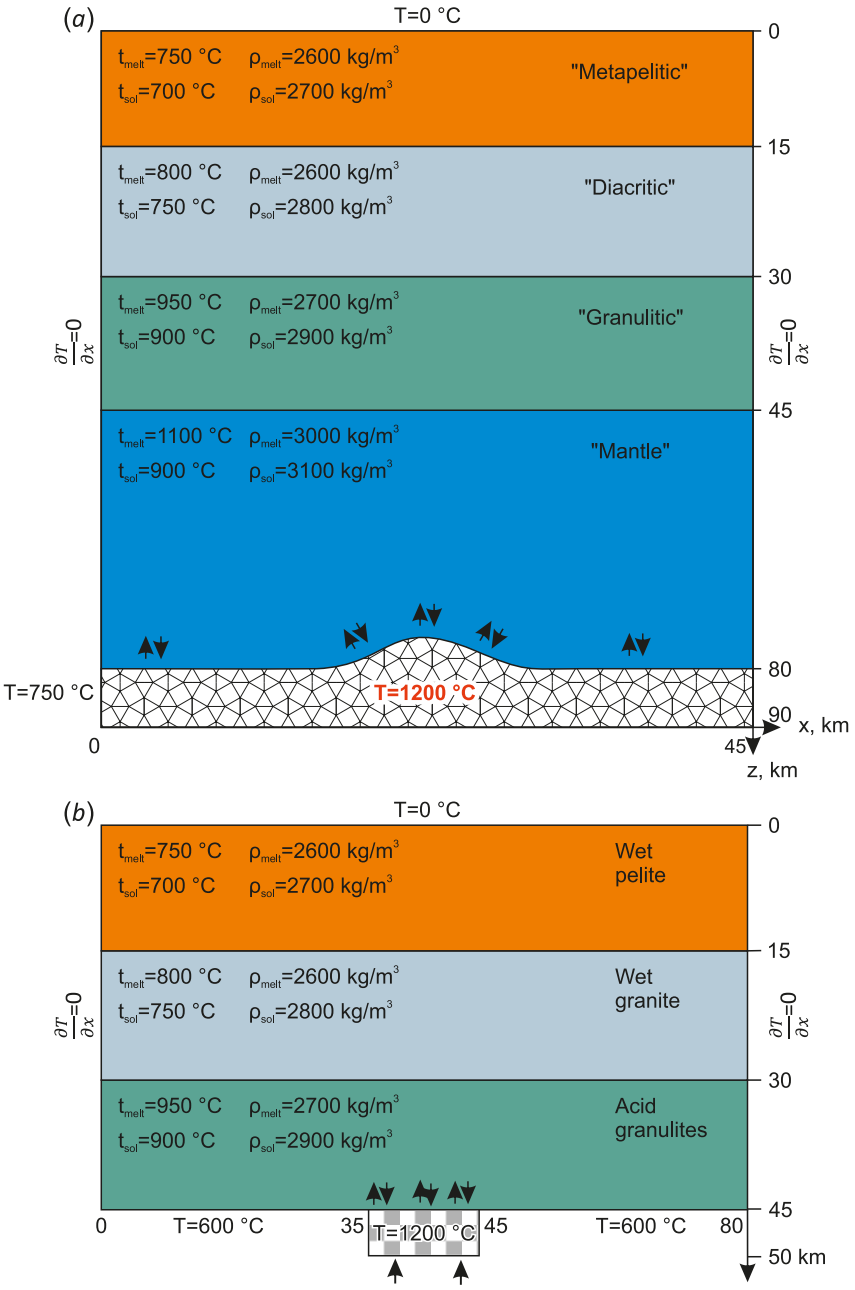

Fig. 6. Scheme of the problem statement. Shown here is the geometry of the computational domain, representing a three-layer crust and temperature boundary conditions.
Melting parameters and melt/solid densities are given for each area. An ornament at the base of the crust shows a magma reservoir in the form of a layer 10 km thick (model *a*) and a conduit 10 km wide (model *b*).

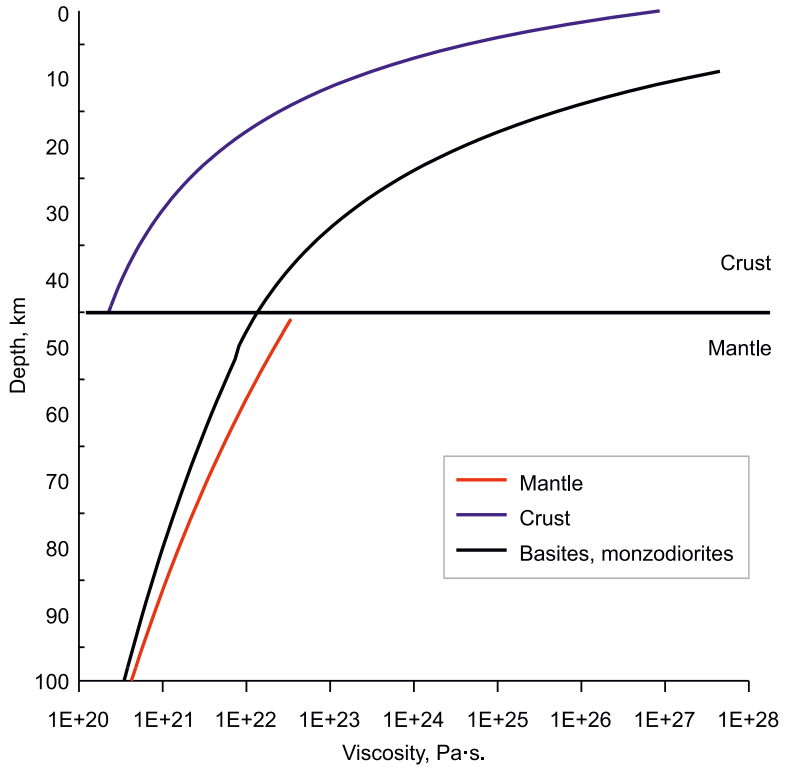

Fig. 7. Dependence of viscosity on depth at a fixed strain rate ($\dot{\varepsilon}_{II} = 10^{-13}\left[1/\mathrm{c}\right]$) for the crustal, mantle and magmatic materials used in the model.

and volatile components) decreases with depth in the (meta) pelite, granite/diorite and granulite layer. Data from [Droop, Brodie, 2012; Nair, Chacko, 2002] were used as melting parameters, on the basis of which melting temperature ranges were set for the metapelite, granite-diorite and granulite layers of the crust. The density and melt fraction varies linearly across the melting range, with a maximum melting degree of 0.75. A stepwise increase in melt/rock density with depth at the boundaries of crustal layers was assumed (Fig. 6). Thermophysical parameters are shown in Fig. 6, 7 and in Table 2.

The system of Navier-Stokes equations for a multiphase medium is solved in the compressible fluid approximation: the continuity equation, the equation of motion and the energy conservation equation. A detailed description of the system of equations used in the model is given in [Semenov, Polyansky, 2017; Polyansky et al., 2021a] and is not repeated here. To solve the problem, the ANSYS Fluent computing package [ANSYS..., 2013] is used, which implements numerical algorithms for solving problems of the flow of nonlinear viscous, temperature-dependent fluid.

5. RESULTS OF MODELING (COLLISIONAL STAGE)

The results of modeling the formation of intrusions of the collision stage 520–490 Ma (stated in Fig. 6, a) with the presence of a deep magma chamber in the form of a horizontal body in the upper mantle are presented in Fig. 8. Model results are shown in the form of density and temperature distributions after 1.5, 3, 12, 32, 62 and 220 kyr from the moment of the magma chamber occurrence.

At the initial stage, the mantle is heated and partially melted, as a result of which the mantle material becomes positively buoyant and begins to rise in the form of a single diapir. During this ascent, the molten. positively buoyant part of the mantle and the mafic melt from the magma chamber rise together and, as they ascent, differentiation of the picritic and mafic melt occurs. A mixture of mafic and peridotite material rises to the level of the lower crust in a mushroom shape with a wide front and a narrow feeding channel. The duration of the magma rise from the source to the crustal boundary takes up to 3 kyr (Fig. 8, "3 kyr"). Further, an intermediate chamber is formed at the crust-mantle boundary. Melting of the lower crustal material occurs above the chamber, it becomes positively buoyant and as a result rises to the level of the middle crust. The mafic material remains in the lower part of the crust and cannot rise higher. The duration of this process takes up to 10 kyr (Fig. 8, "12 kyr'). At the crust-mantle boundary, a region is formed in which the material of the lower crust, upper mantle and mafic-ultrabasic magma is mixed. The boundary itself becomes irregular, and an magma underplating is formed, in which lenses and interlayers of peridotites, mafic rocks, and granulites alternate. Such a compositionally heterogeneous region represents a crust-mantle transition zone according to [O'Reilly, Griffin, 2013].

Next, the melting process is "transmitted" to the upper layers of the crust. A magma chamber is formed at the boundary of the lower and middle crust, melting of the middle crust and rise of magma in the middle crust. The

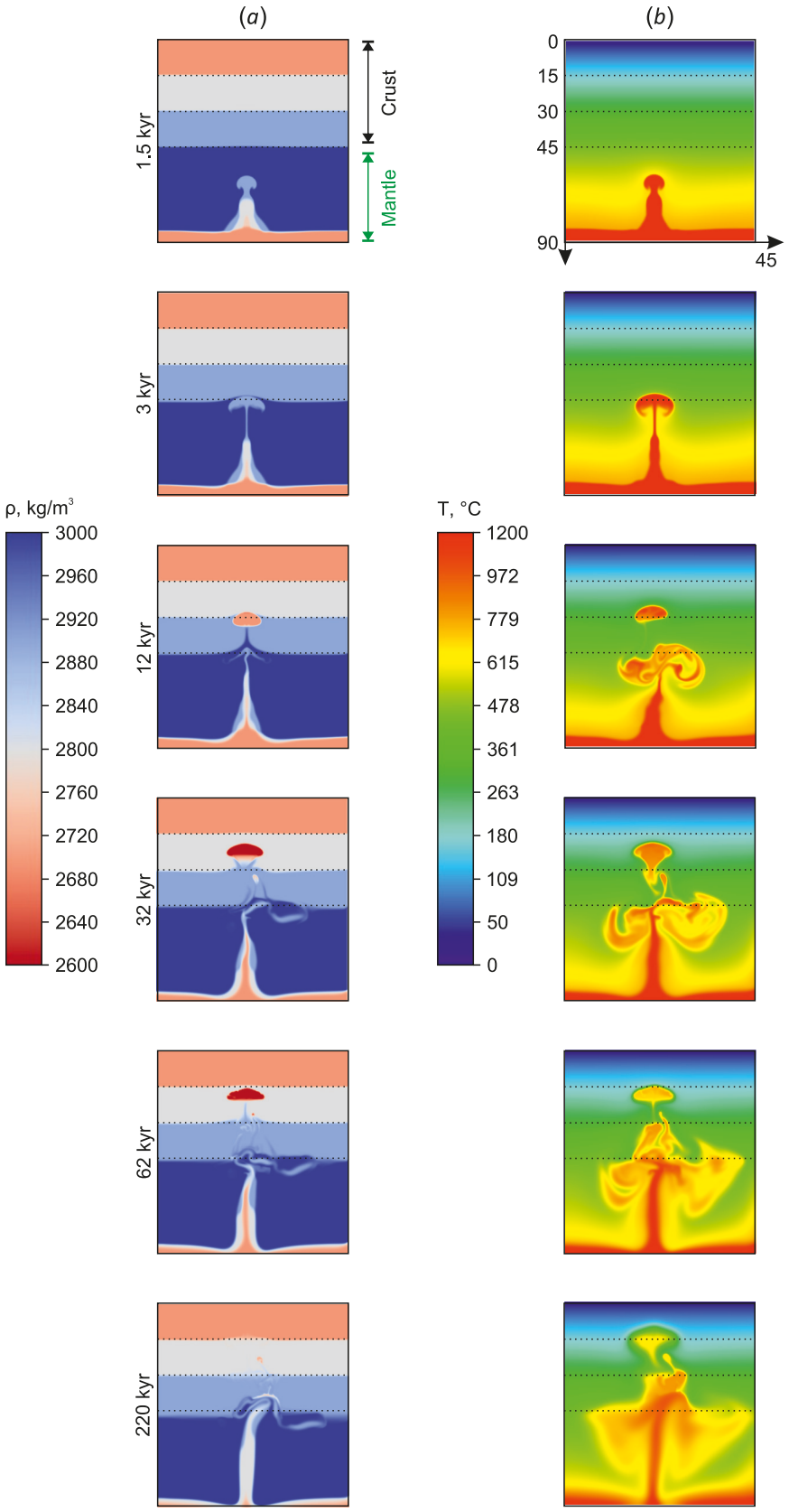

Fig. 8. Results of modeling the formation of collisional mantle-crustal intrusion (520–490 Ma).
There are shown density (*a*) and temperature (*б*) patterns for certain moments of time after the occurrence of magmatic source in the mantle. The density pattern reflects the evolution of rising magma and the composition of host rocks in the mantle and three-layer crust. Dotted lines are density boundaries.

material from the lower crust solidifies at a depth of about 20 km. The active stage of ascent and subsidence lasts up to 50 kyr (Fig. 8, "32 and 62 kyr"). As it cools, the rising process slows down and crystallization occurs. (It is worth noting a feature of visualizing the results of a numerical experiment: in Fig. 8, density inhomogeneities in the crust "disappear" over time due to an increase in density during crystallization, but the frozen substance remains "in place", forming deep crystalline massifs). During the melting and transport of magma in the crust, at the same time, the convective rise of magma continues in the mantle (Fig. 8, "62 and 220 kyr"). The process stops when the deep magma source is depleted and its "feeding" stops or the feeding channel freezes. In this example, a 10-kilometer thick layer is depleted in approximately 200–250 kyr.

Modeling of magmatism at the collision stage showed that basaltic material from a magma chamber can rise to depths of 35–40 km, form an intermediate chamber at the base of the crust, from which further rise occurs together with the melting products of the lower crust, crystallization and the final formation of massifs at the upper-middle crust boundary. The melting product of the lower crust can rise to depths of about 20 km and crystallizes at this level. The duration of the active stage of melting and uplifting takes no more than 50 kyr. This is followed by cooling and crystallization, lasting up to 200–250 kyr.

6. RESULTS OF MODELING (TRANSTENSIONAL STAGE)

The second model of magmatism of the transtensional stage 465–440 Ma (statement is shown in Fig. 6, b) was developed to describe the process of crust-mantle interaction within the tectonic suture separating the Mugur-Chinchilig and Erzin-Naryn blocks. It is assumed that there is a magma chamber located in the channel of the permeable zone of the mantle.

The results are presented in Fig. 9 in the form of evolution of the intrusion shape, the distribution of the volumetric content of mafic magma and the evolution of temperature.

The process of ascent from a vertical magma conduit differs from the case of a horizontal magma chamber because melt enters the chamber from below from a supposed plum-related source [Egorova et al., 2006; Shelepaev et al., 2018]. Mathematically, this is accomplished by maintaining a constant magmatic pressure at the base of the chamber. Based on geological data, we consider the existence of two types of magmas – mafic and diorite – as successive phases of intrusion from a common source. The simultaneous existence of two magmas, we believe, is explained by the fact that diorite magma is formed because of the interaction of mafic melt and felsic crustal material. That is, diorites are hybrid rocks formed during the intrusion of mafic rocks and the melting of felsic crustal rocks. For Western Sangilen and Transbaikalia, the simultaneous existence of mafic and diorite magmas is justified by the widespread development of combined, as well as mingling dikes, which are described in [Burmakina Tsygankov, 2013; Karmysheva et al., 2015; Vladimirov et al., 2017; Litvinovsky et al., 2017; Polyansky et al., 2017]. Moreover, mingling phenomena are characteristic of both collision and transtensional stages, which justifies the existence of two magmas simultaneously.

The entire magma rise can be divided into two stages: 1) when the melt approaches the density or viscous boundary, an intermediate chamber is formed; 2) when the chamber is opened, magma intruded upward from it and a channel is formed that feeds the multi-chamber magma body. These stages are repeated until the substance reaches such a depth that the energy of the uplifted magma is not enough to reach the melting temperature of the host rock.

Our simulation indicate that the substance from the chamber reaches the base of the middle crust in about 5 kyr. Moreover, during the first 4 kyr, the lower layer of the crust warms up, and the process of breakthrough and channel formation itself lasts about 1 kyr. This duration is mean between the diapiric and dike mechanisms of magma transport [Cruden, Weinberg, 2018]. At the boundary of the lower and middle crust, an intermediate chamber is formed, but since the material has a fairly high temperature and correspondingly low density, an "instant" rise (magma penetration) to the upper crust takes place over several kyr. After this, as it cools, the migration processes in the upper crust slow down, and in the middle and lower crust the chambers are maintained due to the replenishment of new portions of melt from the magma source. As the material of the upper crust melts and reaches approximately 10 % of the volume fraction of mafic melt, the process of ascent in the upper crust begins, which lasts approximately 40 kyr. As a result, the substance from the magma chamber enters the upper crust to a depth of 7 km (1.5–2.0 kbar) in a volume ratio of 1 : 2 mafic to diorite components. The process is to some extent similar to mingling, when high-density mafic inclusions rise in a chamber or dike filled with felsic magma by gravitational floating [Semenov, Polyansky, 2017; Polyansky et al., 2017]. As the substance rises from the magma chamber, it assimilates the host crustal material, the composition becomes multiphase, the proportion of primary magma decreases, and contamination increases. Thus, massifs formed at depths of 15–30 km can have a ratio of the volume fraction of gabbroids to diorites from 1: 2 to 3: 4 and additionally contain no more than 5 % of the volume fraction of lower crustal material in the case of a chamber at a depth of 15 km.

Simulations have shown that states with high melt content are mechanically unstable. When the melt fraction reaches 15–20 vol. %, it will tend to separate into dike swarms that penetrate the crust within 25–50 kyr. (Fig. 10). The substance does not rise through a single channel, but many additional ones are formed from each intermediate chamber. Near the surface, the intrusion represents a main stock-like or laccolith body with many apophyses on the upper roof of the massif ("fingers", personal communication from R.A. Shelepaev about the structure of the Pravotarlashkin massif, established from the results of magnetometric survey).

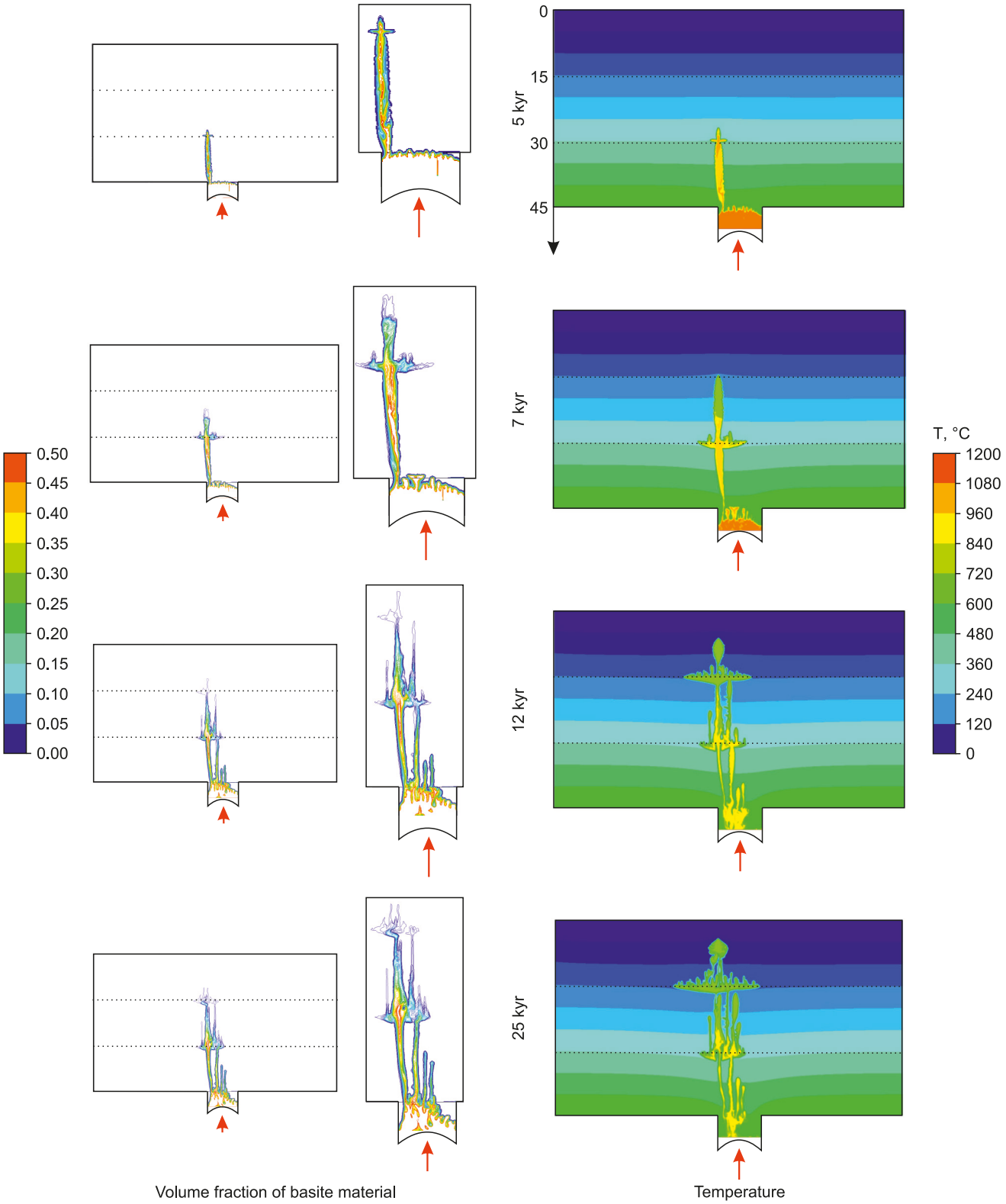

Fig. 9. Results of modeling the formation of a multi-chamber intrusion at the transtensional stage (465–440 Ma).
There are shown the volume fraction of mafic magma (left and central (zoomed image) columns) and temperature (right) distribution for certain moments of time after the beginning of the action of a magmatic source. The scale on the left is the volume fraction of mafic melt in a limited range; the unshaded area in the feeder conduit corresponds to the mafic content higher than 0.5. Dotted lines are density boundaries.

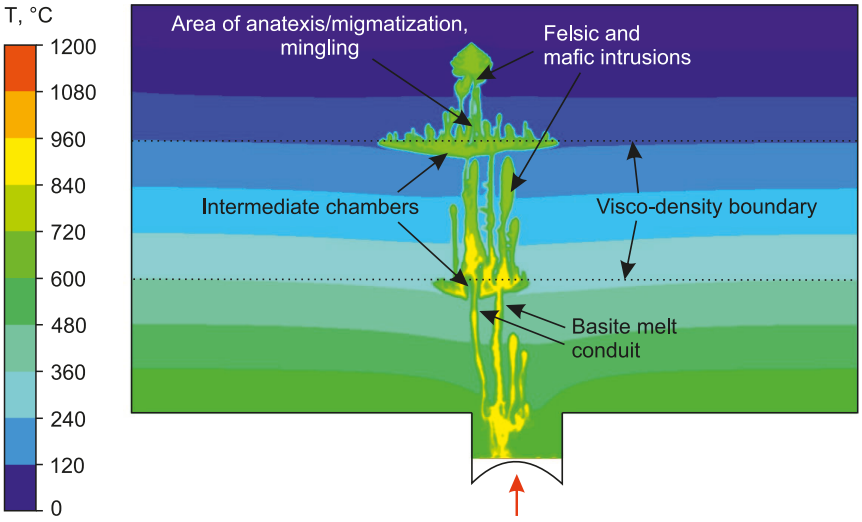

Fig. 10. Scheme of the evolution of a multi-chamber intrusion based on the results of modeling magmatism above a mantle magma conduit.
The details are provided for the structure of the magmatic column formed as a result of melting and transport of mafic magma from the mantle, formation of an intermediate basic source as a result of underplating, melting of the crustal material, hybridization of magma, and formation of the intracrustal massifs.

7. DISCUSSION

Numerical thermomechanical modeling is an effective method for quantitatively describing magmatism processes in different geodynamic settings. The model results show good agreement with the natural petrological characteristics of the formation of multiphase gabbro-granite complexes of the West Sangilen terrane within the Mugur-Chinchilig and Erzin-Naryn blocks.

Geological data and modeling results allow us to draw the following conclusions. The modeling results confirm the close spatial and temporal connection of high-gradient HT/LP type metamorphism with gabbro-monzodiorite formation type intrusions, as well as their two-stage manifestation in Western Sangilen. The model predicts the possibility of the existence of two levels of formation of massifs: low-pressure – Bashkymugur, Pravotarlashkin and deeper – Bayankol, Erzin, Matut massifs, as well as Lower Erzin granulites. It is possible that the mafic magma chamber could be located at a level of about 80 km (2 GPa), near the density boundary of spinel and garnet peridotites. Its composition could correspond to picrite in accordance with the most magnesian compositions of the gabbroids of the Bayankol massif (X_{MgO}=24–25 wt. %, Table 1) with a high (more than 25 %) degree of melting. This area apparently was a magmatic source at the collision stage of the evolution of the Western-Sangilen terrane. At this stage, the Pravotarlashkin, Bayankol, and Erzin massifs were formed. After the source of the low-melting component in the area of magma generation was depleted, magmatism stopped. This was followed by a break in magmatic activity due to the restructuring of the geodynamic regime from collisional to transtensional (shear with extension). At the transtensional stage, the main role as magma conduit was played by deep suture zones, separating individual crustal blocks and penetrating into the upper mantle. At this stage, the Bashkymugur massif was formed, one of the shallow massifs, at the same time having a wide metamorphic zonation of about 5–6 km. The most recent igneous formations – the dikes of the Agardag complex – cut through the rocks of the Pravotarlashkin and Bashkymugur massifs. Data on xenoliths [Egorova et al., 2006] allow to judge the multi-chamber structure of these intrusions, which is confirmed by two-dimensional numerical modeling.

The depth of formation of the ultramafic-mafic massifs of West Sangilen remains a controversial issue, because pressure estimates from mineral geobarometers vary significantly according to data from different authors [Kargopolov, 1997; Karmysheva et al., 2019; Selyatitskii et al., 2021; Azimov et al., 2018; Kozakov, Azimov, 2017]. It is known that the width of the contact areol increases in the case of a more deeply located intrusive body [Reverdatto et al., 2010]. Therefore, the width of metamorphic zoning around igneous bodies characterizes the depth of formation of mafic-ultabasic massifs. The zoning width of the Bayankol (deep) and Bashkymugur (shallow) massifs differs significantly and is 0.5 and 6 km, respectively, which contradicts the indicated pattern. This discrepancy can be explained by the different sizes of the intermediate chambers, which, as follows from the simulation, increases as it approaches the surface (Fig. 10).

8. CONCLUSION

The modeling results allow to establish that material from the magma chamber can reach depths down to the level of the upper crust in volume fractions of gabbroids and diorites from 1:2 to 3:4 and additionally transfer no more than 5 % of lower crustal material. These results explain observations about the actual volumetric ratios of gabbroids and monzodiorites in specific massifs of West Sangilen, in which diorites significantly predominate over gabbroids.

The models develop the well-known idea about the mechanism of generation of granitic magmas due to intrusions of basaltic magmas into the continental crust [Huppert, Sparks, 1988] in relation to the generation of intermediate chambers at the boundaries of continental crust. Density and material boundaries are physical barriers during the formation of intermediate chambers.

Model experiments confirm petrological data on the presence of multi-level chambers during the formation of the Pravotarlashkin and Bashkymugur massifs. Our simulations of collision-stage magmatism indicates that basaltic melt from the upper mantle chamber can form an intermediate chamber at the base of the crust, causing melting of the lower crust, mixing of crustal and mantle material, and the formation of polyphase massifs in the upper-middle crust. The proposed model of transtensional magmatism explains the mechanism of the magma rise along a permeable tectonic zone (magma-conducting channel) in the mantle lithosphere and crust. Such zones of the Sangilen fragment of the Caledonides are the boundaries between the Muguro-Chinchilig and Erzin-Naryn blocks.

The depth of formation and structure of the West Sangilen massifs are apparently determined by a change in the geodynamic regime. This interpretation of the stages of magmatism does not contradict geochemical data on a change in the source, which at the first stage represented a depleted mantle [Shelepaev et al., 2018]. At the transtensional shear stage, the source changed to a deeper and enriched compared to the over-subduction mantle.

9. ACKNOWLEDGEMENTS

The authors express their gratitude to the reviewers, A.E. Izokh, Dr. Sci. (Geol.-Min.), and R.A. Shelepaev, Cand. Sci. (Geol.-Min.), for their useful contributions and comments.

10. CONTRIBUTION OF THE AUTHORS

Both authors made an equivalent contribution to this article, read and approved the final manuscript.

11. DISCLOSURE

Both authors declare that they have no conflicts of interest relevant to this manuscript.

12. REFERENCES

ANSYS Fluent Theory Guide, 2013. Release 15.0. ANSYS Inc., USA, 779 p.

Azimov P.Y., Kozakov I.K., Glebovitsky V.A., 2018. Early Paleozoic UHT/LP Metamorphism in the Sangilen Block of the Tuvino-Mongolian Massif. Doklady Earth Sciences 479, 295–299. https://doi.org/10.1134/S1028334X18030145.

Babichev A.V., Polyansky O.P., Korobeynikov S.N., Reverdatto V.V., 2014. Mathematical Modeling of Magma Fracturing and Dike Formation. Doklady Earth Sciences 458, 1298–1301. https://doi.org/10.1134/S1028334X14100262.

Bea F., 2012. The Sources of Energy for Crustal Melting and the Geochemistry of Heat-Producing Elements. Lithos 153, 278–291. https://doi.org/10.1016/j.lithos.2012.01.017.

Burmakina G.N., Tsygankov A.A., 2013. Mafic Microgranular Enclaves in Late Paleozoic Granitoids in the Burgasy Quartz Syenite Massif, Western Transbaikalia: Composition and Petrogenesis. Petrology 21, 280–303. https://doi.org/10.1134/S086959111303003X.

Carter N.L., Tsenn M.C., 1987. Flow Properties of Continental Lithosphere. Tectonophysics 136 (1–2), 27–63. https://doi.org/10.1016/0040-1951(87)90333-7.

Chopra P.N., Patterson M.S., 1984. The Role of Water in the Deformation of Dunite. Journal of Geophysical Research: Solid Earth 89 (B9), 7861–7876. https://doi.org/10.1029/JB089iB09p07861.

Cruden A.R., Weinberg R.F., 2018. Mechanisms of Magma Transport and Storage in the Lower and Middle Crust – Magma Segregation, Ascent and Emplacement. In: S. Burchardt (Ed.), Volcanic and Igneous Plumbing Systems. Understanding Magma Transport, Storage, Evolution in the Earth's Crust. Elsevier, p. 13–53. http://doi.org/10.1016/B978-0-12-809749-6.00002-9.

Droop G.T.R., Brodie K.H., 2012. Anatectic Melt Volumes in the Thermal Aureole of the Etive Complex, Scotland: The Roles of Fluid-Present and Fluid-Absent Melting. Journal of Metamorphic Geology 30 (8), 843–864. https://doi.org/10.1111/j.1525-1314.2012.01001.x.

Egorova V.V., Volkova N.I., Shelepaev R.A., Izokh A.E., 2006. The Lithosphere beneath the Sangilen Plateau, Siberia: Evidence from Peridotite, Pyroxenite and Gabbro Xenoliths from Alkaline Basalts. Mineralogy and Petrology 88, 419–441. https://doi.org/10.1007/s00710-006-0121-0.

Fedorovsky V.S., Vladimirov A.G., Khain E.V., Kargopolov S.A., Gibsher A.S., Izokh A.E., 1995. Tectonics, Metamorphism, and Magmatism of Collision Zones in Early Paleozoic Orogenic Complexes of Central Asia. Geotectonics 3, 3–22 (in Russian) [Федоровский В.С., Владимиров А.Г., Хаин Е.В., Каргополов С.А., Гибшер А.С., Изох А.Э. Тектоника, метаморфизм и магматизм коллизионных зон каледонид Центральной Азии // Геотектоника. 1995. Т. 29. № 3. С. 3–22].

Ghiorso M.S., Gualda G.A.R., 2015. An H_2O-CO_2 Mixed Fluid Saturation Model Compatible with Rhyolite-MELTS. Contributions to Mineralogy and Petrology 169, 53. https://doi.org/10.1007/s00410-015-1141-8.

Gibsher A.A., Malkovets V.G., Travin A.V., Sharygin V.V., Belousova E.A., Konc Z., 2012. The Age of Camptonite Dikes of the Agardag Alkali-Basalt Complex (Western Sangilen): Results of Ar/Ar and U/Pb Dating. Russian Geology and Geophysics 53 (8), 763–775. https://doi.org/10.1016/j.rgg.2012.06.004.

Gibsher A.S., Gibsher A.A., Malkovets V.G., Shelepaev R.A., Terleev A.A., Sukhorukov V.P., Rudnev S.N., 2017. The Nature and Age of High-Pressure (Kyanite) Metamorphism of the Western Sangilen (Southeastern Tuva). In: Geodynamic Settings and Thermodynamic Conditions of Regional Metamorphism in the Precambrian and Phanerozoic. Proceedings of the V Russian Conference on Precambrian Geology and Geodynamics (October 24–26, 2017). IPGG RAS,

Saint-Petersburg, p. 52–53 (in Russian) [Гибшер А.С., Гибшер А.А., Мальковец В.Г., Шелепаев Р.А., Терлеев А.А., Сухоруков В.П., Руднев С.Н. Природа и возраст высокобарического (кианитового) метаморфизма Западного Сангилена (Юго-Восточная Тува) // Геодинамические обстановки и термодинамические условия регионального метаморфизма в докембрии и фанерозое: Материалы V Российской конференции по проблемам геологии и геодинамики докембрия (24–26 октября 2017 г.). СПб.: ИГГД РАН, 2017. С. 52–53].

Gualda G.A.R., Ghiorso M.S., Lemons R.V., Carley T.L., 2012. Rhyolite-MELTS: A Modified Calibration of MELTS Optimized for Silica-Rich, Fluid-Bearing Magmatic Systems. Journal of Petrology 53 (5), 875–890. https://doi.org/10.1093/petrology/egr080.

Huppert H.E., Sparks R.S.J., 1988. The Generation of Granitic Magmas by Intrusion of Basalt into Continental Crust. Journal of Petrology 29 (3), 599–624. https://doi.org/10.1093/petrology/29.3.599.

Izokh A.E., Kargopolov S.A., Shelepaev R.A., Travin A.V., Egorova V.V., 2001. Cambrian-Ordovician Basite Magmatism of the Altai-Sayan Folded Area and Its Related Metamorphism with High Temperatures and Low Pressures. In: Actual Problems of Geology and Minerageny of the Southern Siberia. Proceedings of the Scientific and Practical Conference (October 31 – November 2, 2001, Elan, Novokuznetsk district, Kemerovo Region). LIH SB RAS, Novosibirsk, p. 68–72 (in Russian) [Изох А.Э., Каргополов С.А., Шелепаев Р.А., Травин А.В., Егорова В.В. Базитовый магматизм кембро-ордовикского этапа Алтае-Саянской складчатой области и связь с ним метаморфизма высоких температур и низких давлений // Актуальные вопросы геологии и минерагении юга Сибири: Материалы научно-практической конференции (31 октября – 2 ноября 2001 г., пос. Елань Новокузнецкого района, Кемеровской области). Новосибирск: Изд-во ИГиЛ СО РАН, 2001. С. 68–72].

Kargopolov S.A., 1991. Metamorphism of the Mugur Zonal Complex (Southeastern Tuva). Russian Geology and Geophysics 32 (3), 109–119 (in Russian) [Каргополов С.А. Метаморфизм мугурского зонального комплекса (Юго-Восточная Тува) // Геология и геофизика. 1991. Т. 32. № 3. С. 109–119].

Kargopolov S.A., 1997. Shallow-Depth Granulites of the Western Sangilen (Southeastern Tuva). PhD Thesis (Candidate of Geology and Mineralogy). Novosibirsk, 272 p. (in Russian) [Каргополов С.А. Малоглубинные гранулиты Западного Сангилена (Юго-Восточная Тува): Дис. ... канд. геол.-мин. наук. Новосибирск, 1997. 272 с.].

Karmysheva I.V., Vladimirov V.G., Shelepaev R.A., Rudnev S.N., Yakovlev V.A., Semenova D.V., 2019. Bayan-Kol Gabbro-Granite Association (Western Sangilen, Southeastern Tuva): Composition, Age Boundaries, and Tectonic and Geodynamic Settings. Russian Geology and Geophysics 60 (7), 720–734. https://doi.org/10.15372/RGG2019065.

Karmysheva I.V., Vladimirov V.G., Vladimirov A.G., Shelepaev R.A., Yakovlev V.A., Vasyukova E.A., 2015. Tectonic Position of Mingling Dykes in Accretion-Collision System of Early Caledonides of West Sangilen (South-East Tuva, Russia). Geodynamics & Tectonophysics 6 (3), 289–310 (in Russian) [Кармышева И.В., Владимиров В.Г., Владимиров А.Г., Шелепаев Р.А., Яковлев В.А., Васюкова Е.А. Тектоническая позиция минглинг-даек в аккреционно-коллизионной системе ранних каледонид Западного Сангилена (Юго-Восточная Тува) // Геодинамика и тектонофизика. 2015. Т. 6. № 3. С. 289–310]. https://doi.org/10.5800/GT-2015-6-3-0183.

Keller T., May D.A., Kaus B.J.P., 2013. Numerical Modelling of Magma Dynamics Coupled to Tectonic Deformation of Lithosphere and Crust. Geophysical Journal International 195 (3), 1406–1442. https://doi.org/10.1093/gji/ggt306.

Kozakov I.K., Azimov P.Y., 2017. Geodynamics of the Origin of Granulites in the Sangilen Block of the Tuva-Mongolian Terrane, Central Asian Orogenic Belt. Petrology 25, 615–624. https://doi.org/10.1134/S0869591117060042.

Kozakov I.K., Kotov A.B., Sal'nikova E.B., Kovach V.P., Natman A., Bibikova E.V., Kirnozova T.I., Todt W., Kröner A., Yakovleva S.Z., Lebedev V.I., Sugorakova A.M., 2001. Timing of the Structural Evolution of Metamorphic Rocks in the Tuva-Mongolia Massif. Geotectonics 35 (3), 165–184.

Kozakov I.K., Sal'nikova E.B., Kotov A.B., Kovach V.P., Bibikova E.V., Kirnozova T.I., 1999. Polychronous Evolution of the Paleozoic Granitoid Magmatism in the Tuva-Mongolia Massif: U-Pb Geochronological Data. Petrology 7 (6), 592–601.

Kronenberg A.K., Tullis J., 1984. Flow Strength of Quartz Aggregates: Grain Size and Pressure Effects Due to Hydrolytic Weakening. Journal of Geophysical Research: Solid Earth 89 (B6), 4281–4297. https://doi.org/10.1029/JB089iB06p04281.

Kuznetsova L.G., Shokalsky S.P., Sergeev S.A., Dril S.I., 2021. Age and Composition of the Early Paleozoic Magmatic Associations and Related Rare-Element Pegmatites in the South-Eastern Part of the Sangilen Block, Tuva-Mongolian Massif. Geodynamics & Tectonophysics 12 (2), 261–286 (in Russian) [Кузнецова Л.Г., Шокальский С.П., Сергеев С.А., Дриль С.И. Возрастные рубежи проявления и особенности состава раннепалеозойского магматизма и связанных с ним редкометалльных пегматитов в юго-восточной части Сангиленского блока Тувино-Монгольского массива // Геодинамика и тектонофизика. 2021. Т. 12. № 2. С. 261–286. https://doi.org/10.5800/GT-2021-12-2-0524.

Litvinovsky B.A., Zanvilevich A.N., Wickham S.M., Jahn B.M., Vapnik Y., Kanakin S.V., Karmanov N.S., 2017. Composite Dikes in Four Successive Granitoid Suites from Transbaikalia, Russia: The Effect of Silicic and Mafic Magma Interaction on the Chemical Features of Granitoids. Journal of Asian Earth Sciences 136, 16–39. https://doi.org/10.1016/j.jseaes.2016.12.037.

Marsh B.D., 1982. On the Mechanics of Igneous Diapirism, Stoping, and Zone Melting. American Journal of Science 282 (6), 808–855. https://doi.org/10.2475/ajs.282.6.808.

Mei S., Bai W., Hiraga T., Kohlstedt D.L., 2002. Influence of Melt on the Creep Behavior of Olivine-Basalt Aggregates

under Hydrous Conditions. Earth and Planetary Science Letters 201 (3–4), 491–507. https://doi.org/10.1016/S0012-821X(02)00745-8.

Nair R., Chacko T., 2002. Fluid-Absent Melting of High-Grade Semi-Pelites: P-T Constraints on Orthopyroxene Formation and Implications for Granulite Genesis. Journal of Petrology 43 (11), 2121–2142. https://doi.org/10.1093/petrology/43.11.2121.

Nimis P., 2002. Clinopyroxene Geobarometry of Magmatic Rocks. Structural Geobarometers for Basic to Acid, Tholeiitic and Mildly Alkaline Magmatic Systems. Contributions to Mineralogy and Petrology 135, 62–74. https://doi.org/10.1007/s004100050498.

O'Reilly S.Y., Griffin W.L., 2013. Moho vs Crust-Mantle Boundary: Evolution of an Idea. Tectonophysics 609, 535–546. https://doi.org/10.1016/j.tecto.2012.12.031.

Persikov E.S., 1984. Viscosity of Magmatic Melts. Nauka, Moscow, 159 p. (in Russian) [Персиков Э.С. Вязкость магматических расплавов. М.: Наука, 1984. 159 с.].

Persikov E.S., Bukhtiyarov P.G., 2009. Interrelated Structural Chemical Model to Predict and Calculate Viscosity of Magmatic Melts and Water Diffusion in a Wide Range of Compositions and T-P Parameters of the Earth's Crust and Upper Mantle. Russian Geology and Geophysics 50 (12), 1079–1090. https://doi.org/10.1016/j.rgg.2009.11.007.

Petrova A.Yu., Kostitsyn Yu.A., 1997. Age of High-Gradient Metamorphism and Granite Formation in Western Sangilen. Geochemistry 3, 343–347 (in Russian) [Петрова А.Ю., Костицын Ю.А. Возраст высокоградиентного метаморфизма и гранитообразования на Западном Сангилене // Геохимия. 1997. № 3. С. 343–347].

Polyansky O.P., Babichev A.V., Semenov A.N., Reverdatto V.V., 2021a. Modelling Heat Generation during Friction and Viscoplastic Deformation Based on the Example of the Yenisei Shear Zone (Eastern Siberia). Geodynamics & Tectonophysics 12 (4), 909–928 (in Russian) [Полянский О.П., Бабичев А.В., Семенов А.Н., Ревердатто В.В. Моделирование теплогенерации при трении и вязкопластической деформации на примере Приенисейской сдвиговой зоны (Восточная Сибирь) // Геодинамика и тектонофизика. 2021. Т. 12. № 4. С. 909–928]. https://doi.org/10.5800/GT-2021-12-4-0563.

Polyansky O.P., Izokh A.E., Semenov A.N., Selyatitskii A.Y., Shelepaev R.A., Egorova V.V., 2021b. Thermomechanical Modeling of the Formation of Multi-Chamber Intrusions for Identifying the Relationship of Plutonic Metamorphism with Gabbro-Diorite Massifs of Western Sangilen, Tuva, Russia. Geotectonics 55, 1–19. https://doi.org/10.1134/S001685212101009X.

Polyansky O.P., Kargopolov S.A., Izokh A.E., Semenov A.N., Babichev A.V., Vasilevsky A.N., 2019. The Role of Magmatic Heat Sources in the Formation of Regional and Contact Metamorphic Areas in West Sangilen (Tuva, Russia). Geodynamics & Tectonophysics 10 (2), 309–323 (in Russian) [Полянский О.П., Каргополов С.А., Изох А.Е., Семенов А.Н., Бабичев А.В., Василевский А.Н. Роль магматических источников тепла при формировании регионального и контактовых метаморфических ареалов Западного Сангилена (Тува) // Геодинамика и тектонофизика. 2019. Т. 10. № 2. С. 309–323]. https://doi.org/10.5800/GT-2019-10-2-0416.

Polyansky O.P., Semenov A.N., Vladimirov V.G., Karmysheva I.V., Vladimirov A.G., Yakovlev V.A., 2017. Numerical Simulation of Magma Mingling (Case of Bayankol Gabbro-Granite Series, Sangilen, Tuva). Geodynamics & Tectonophysics 8 (2), 385–403 (in Russian) [Полянский О.П., Семенов А.Н., Владимиров В.Г., Кармышева И.В., Владимиров А.Г., Яковлев В.А. Численная модель магматического минглинга (на примере баянкольской габбро-гранитной серии, Сангилен, Тува) // Геодинамика и тектонофизика. 2017. Т. 8. № 2. С. 385–403]. https://doi.org/10.5800/GT-2017-8-2-0247.

Reverdatto V.V., Babichev A.V., Korobeinikov S.N., Polyanskii O.P., 2010. Estimation of the Emplacement Depth of a Magmatic Intrusive Body Based on the Data for Distribution of Isograds in the Surrounding Metamorphic Zoning (Model Approximation). Doklady Earth Sciences 430, 244–247. https://doi.org/10.1134/S1028334X10020212.

Schmeling H., Marquart G., Weinberg R., Wallner H., 2019. Modelling Melting and Melt Segregation by Two-Phase Flow: New Insights into the Dynamics of Magmatic Systems in the Continental Crust. Geophysical Journal International 217 (1), 422–450. https://doi.org/10.1093/gji/ggz029.

Selyatitskii A.Yu., Polyansky O.P., Shelepaev R.A., 2021. A High-Pressure Thermal Aureole of the Bayankol Gabbro-Monzodiorite Intrusion (Western Sangilen, Southeastern Tuva): Evidence for Lower-Crust Mafic Magma Chambers. Russian Geology and Geophysics 62 (9), 987–1005. https://doi.org/10.2113/RGG20194157.

Semenov A.N., Polyansky O.P., 2017. Numerical Modeling of the Mechanisms of Magma Mingling and Mixing: A Case Study of the Formation of Complex Intrusions. Russian Geology and Geophysics 58 (11), 1317–1332. https://doi.org/10.1016/j.rgg.2017.11.001.

Shelepaev R.A., Egorova V.V., Izokh A.E., Seltmann R., 2018. Collisional Mafic Magmatism of the Fold-Thrust Belts Framing Southern Siberia (Western Sangilen, Southeastern Tuva). Russian Geology and Geophysics 59 (5), 525–540. https://doi.org/10.1016/j.rgg.2018.04.006.

Smolyakova A.E., Vladimirov V.G., Karmysheva I.V., Yakovlev V.A., 2021. The Syncollisional Formation Stage of the Bayan-Kol Gabbro-Granodiorite-Granite Massif: on the Basis of the Analysis of Mafic Magmatic Inclusions (Northwestern Margin of the Tuva-Mongolia Massif). In: Petrology and Geodynamics of Geoloical Processes. Proceedings of the XIIth All-Russian Petrographic Meeting with International Participation (September 6–13, 2021). Vol. 3. Publishing House of the Sochava Institute of Geography SB RAS, Irkutsk, p. 83–84 (in Russian) [Смолякова А.Е., Владимиров В.Г., Кармышева И.В., Яковлев В.А. Становление синколлизионного Баянкольского габбро-гранодиорит-гранитного массива: на основе анализа мафических магматических включений (северо-западная окраина Тувино-Монгольского массива) // Петрология и геодинамика геологических процессов: Материалы XII всероссийского петрографического совещания с участием

зарубежных ученых (6–13 сентября, 2021 г.). Иркутск: Изд-во Института географии им. В.Б. Сочавы СО РАН, 2021. Т. 3. С. 83–84].

Vasilevsky A.N., Boldyrev M.A., Mikheev V.V., Dergachev A.A., Krasavin V.V., Kirin Yu.M., Fomin Yu.N., Filina A.G., Blagovidova T.Ya., Kuchai O.A., 1985. Scientific and Technical Report of the Altai-Sayan Experimental-Methodological Seismological Expedition. Institute of Geology and Geophysics, Siberian Branch of the USSR Academy of Sciences, Novosibirsk, 243 p. (in Russian) [Василевский А.Н., Болдырев М.А., Михеев В.В., Дергачев А.А., Красавин В.В., Кирин Ю.М., Фомин Ю.Н., Филина А.Г., Благовидова Т.Я., Кучай О.А. Научно-технический отчет Алтае-Саянской опытно-методической сейсмологической экспедиции. Новосибирск: ИГиГ СО АН СССР, 1985. 243 с.].

Vladimirov V.G., Karmysheva I.V., Yakovlev V.A., Travin A.V., Tsygankov A.A., Burmakina G.N., 2017. Thermochronology of Mingling Dykes in West Sangilen (South-East Tuva, Russia): Evidence of the Collapse of the Collisional System in the North-Western Edge of the Tuva-Mongolia Massif. Geodynamics & Tectonophysics 8 (2) 283–310 (in Russian) [Владимиров В.Г., Кармышева И.В., Яковлев В.А., Травин А.В., Цыганков А.А., Бурмакина Г.Н. Термохронология минглинг-даек Западного Сангилена (Юго-Восточная Тува): свидетельства развала коллизионной системы на северо-западной окраине Тувино-Монгольского массива // Геодинамика и тектонофизика. 2017. Т. 8. № 2. С. 283–310]. https://doi.org/10.5800/GT-2017-8-2-0242.

Vladimirov V.G., Vladimirov A.G., Gibsher A.S., Travin A.V., Rudnev S.N., Shemelina I.V., Barabash N.V., Savinykh Ya.V., 2005. Model of the Tectonometamorphic Evolution for the Sangilen Block (Southeastern Tuva, Central Asia) as a Reflection of the Early Caledonian Accretion – Collision Tectogenesis. Doklady Earth Sciences 405 (8), 1159–1165.